ELSEVIER

Contents lists available at ScienceDirect

Quaternary International

journal homepage: www.elsevier.com/locate/quaint





Luminescence ages and new interpretations of the timing and deposition of Quaternary sediments at Natural Trap Cave, Wyoming

Shannon Mahan ^{a,*}, John R. Wood ^b, David M. Lovelace ^c, Juan Laden ^d, Jenny L. McGuire ^{e,f,g}, Julie A. Meachen ^h

- a Department of Interior, U.S. Geological Survey, Denver Federal Center, Bldg 95, Luminescence Geochronology Lab, Denver, CO, 80225, USA
- ^b Department of Interior, National Park Service, Geologic Resources Division, Lakewood, CO, 80235, USA
- ^c University of Wisconsin-Madison, Dept. of Geoscience, UW Geology Museum, 1215 W. Dayton Street, Madison, WI, 53706, USA
- ^d Tomatoe Salvage, Welding and Rigging, Lander, WY, 82520, USA
- e School of Biological Sciences, Georgia Institute of Technology, 311 Ferst Dr NW, Atlanta, GA, 30332, USA
- f School of Earth and Atmospheric Sciences, Georgia Institute of Technology, 311 Ferst Dr NW, Atlanta, GA, 30332, USA
- g Interdisciplinary Graduate Program in Quantitative Biosciences, Georgia Institute of Technology, 311 Ferst Dr NW, Atlanta, GA, 30332, USA
- h Des Moines University, Dept. of Anatomy, 3200 Grand Ave, Des Moines, IA, 50312, USA

ARTICLE INFO

Keywords: Luminescence dating Tephrochronology Fission track dating Argon dating Geochronology Natural Trap Cave

ABSTRACT

Natural Trap Cave, located in the Big Horn Mountains of north-central Wyoming, has a history of trapping and preserving a range of North American fauna that plummeted into the deep vertical entrance. These animal remains were buried and preserved within sediments of the main chamber and, in turn, have helped elucidate the procession of faunal dynamics during the latest glacial cycle. The cave location, south of the Laurentide and Cordilleran Ice Sheets, and proximal to Yellowstone, is at an ideal geographical juncture to provide insights to ecological changes in North America. The sediments that the animals are buried in inform us about transport and deposition both inside and outside of the cave that relate to catchment dynamics. We report on a series of optically stimulated luminescence (OSL) ages derived from samples obtained within the cave during excavation work in 2014 and in 2018. We also examine chronology produced by argon, tephrochronology, fission track, and luminescence techniques that have been used for understanding the infilling of the cave. The cave sediment ages and in situ measured gamma spectroscopy as measured in this study helped resolve an improved chronological age model when combined with previous data.

The suite of OSL ages is interpreted through the stratigraphic relationships (and vertebrates contained within) which requires the use of an adequate age model; we use either the central age model or minimum age model where appropriate and with justification. Lowest sediments are dated to $\sim\!150$ ka with a hiatus at $\sim\!130$ to 52 ka. Above this, sediment deposition and entrainment of paleontological materials are representative of Pleistocene and early Holocene times, between 37 ± 6 ka and 7.6 ± 0.5 ka. The stratigraphic architecture suggests that deposition of materials into the cave is episodic and rapid, followed by quiescent periods where hydrologic scour, heavy overland flow, or possibly a cryo-hydrologic process may have altered unit relationships. Thus, the complementary geochronometers and the characteristics of quartz versus feldspar luminescence signals improve temporal interpretations of these complex deposits. This adapted understanding of mixing also sets the stage for future work with the aim to improve our understanding of ages and sources for ash units within these cave deposits. The three ash units recognized in the cave may represent an in-situ reworking of the same ash or may be representative of previously undocumented eruptions from the Yellowstone Caldera.

1. Introduction

Natural Trap Cave (NTC) is located northeast of Lovell, Wyoming,

USA on the edge of a plateau in the northern Bighorn Mountains at an elevation of 1,512 m (4,960 ft) (Fig. 1). Geographically, the cave is positioned south of a gap that developed between the Laurentide and

E-mail address: smahan@usgs.gov (S. Mahan).

^{*} Corresponding author.

Cordilleran ice sheets in central North America at the end of the Last Glacial Maximum (LGM) ~15-14,500 cal ka BP (Dyke, 2003). The cave contains exceptionally well preserved and diverse faunal specimens that span the last 150 ka, although the large majority of dated remains are younger than 35 cal ka BP. Of the specimens collected and dated, the majority lived during the Pinedale glaciation, which lasted from approximately 30 to 11.5 ka (Nelson et al., 1979; Benson et al., 2005). The known ages of large Pleistocene animal remains found in the cave has primarily been a result of direct radiocarbon dating of the bones, a dozen or so luminescence ages, and various isotopic methods of dating and elemental concentration analyses on layers of ash preserved in the sediments. Volcanic ash occurs in three distinct layers within the cave sediments deposited during the late Pleistocene (Lovelace et al., this issue; Minkley et al., this issue). This manuscript presents a new luminescence geochronology based within the stratigraphy of the 2014–2018 work by David Lovelace (Lovelace et al., this volume; Fig. 2).

The earliest scientific excavations at NTC lasted for an 11-year period between 1973 and 1985 (Martin and Gilbert, 1978; Wang and Martin, 1993). After a 30-year hiatus, fieldwork at NTC resumed in 2014, leading to new insights into paleobiogeography, depositional history, phylogeny, updated geochronology of cave sedimentation, and detailed stratigraphic framework, control, and description (Lovelace et al., this issue; Fig. 2). Our overall goal is to establish an improved geochronological framework of individual Quaternary sedimentary units at the site, preserve archival chronology, determine the means of sediment transport for the dated layers in the cave, and speculate on the various methodological complexities inherent in the dates of the volcanic ashes. In consideration of this goal, we will 1) evaluate the overall geochronology and stratigraphy inconsistencies for temporal assignments, 2) review the three chronometers used in the 1970's to date the fossils and environmental markers (directly or indirectly). This includes the suite of bulk radiocarbon on organic remains, fission track on minerals in ash, and thermoluminescence (TL) on feldspars contained in the ash, and to 3) report previous and assess newly acquired data, including: optically stimulated luminescence (OSL) ages from sediment in the cave, argon dating of minerals in the middle volcanic ash, tephrochronology of the upper ash (analyses of the chemical fingerprints) and supplement these data with radiocarbon age assessments and U/Pb isotopic dates on the lower ash (Schmitt et al., this issue) from newly recovered material.

1.1. Geological setting

The Bighorn Mountains are a north-south to northwest trending Laramide structure, flanked by late Paleozoic through Mesozoic sedimentary sequences (Fig. 1). The western slope of the mountains hosts a number of known caves, including NTC on what is called the Little Mountain Plateau. The entrance for NTC is situated on a narrow ridge that slopes westward and is flanked by deeply incised ephemeral surface drainages. The cave itself is approximately 24.5 m deep at the largest entrance. Recent mapping of the cave found several sediment-filled passages located high along the margins of the main chamber. A very large 'lower chamber' with an opening originally discovered during the 1985 excavation (Wang and Martin, 1993) was not included in the 2016 DistoX survey but was incorporated in the 2016 LiDAR survey and surveyed again in 2021 (see Lovelace et al., this issue). This lower chamber also contains sediment and Pleistocene fossils, however it is unknown if the inputs to this chamber were co-depositional with the materials in the overlying room where previous excavations have been focused or were subsequently transported due to disturbance or natural processes (Wang and Martin, 1993; Lovelace et al., this issue). Preliminary examination of the sediment and fossils within the lower chamber during the 2021 expedition identified disarticulated bones on top of and within a damp fine-grained matrix of poorly differentiated lithology, indicating that remobilization and transport of materials occurs to lower levels in the cave (Lovelace et al., this issue; Murphy et al., 2001; Bull, 1981).

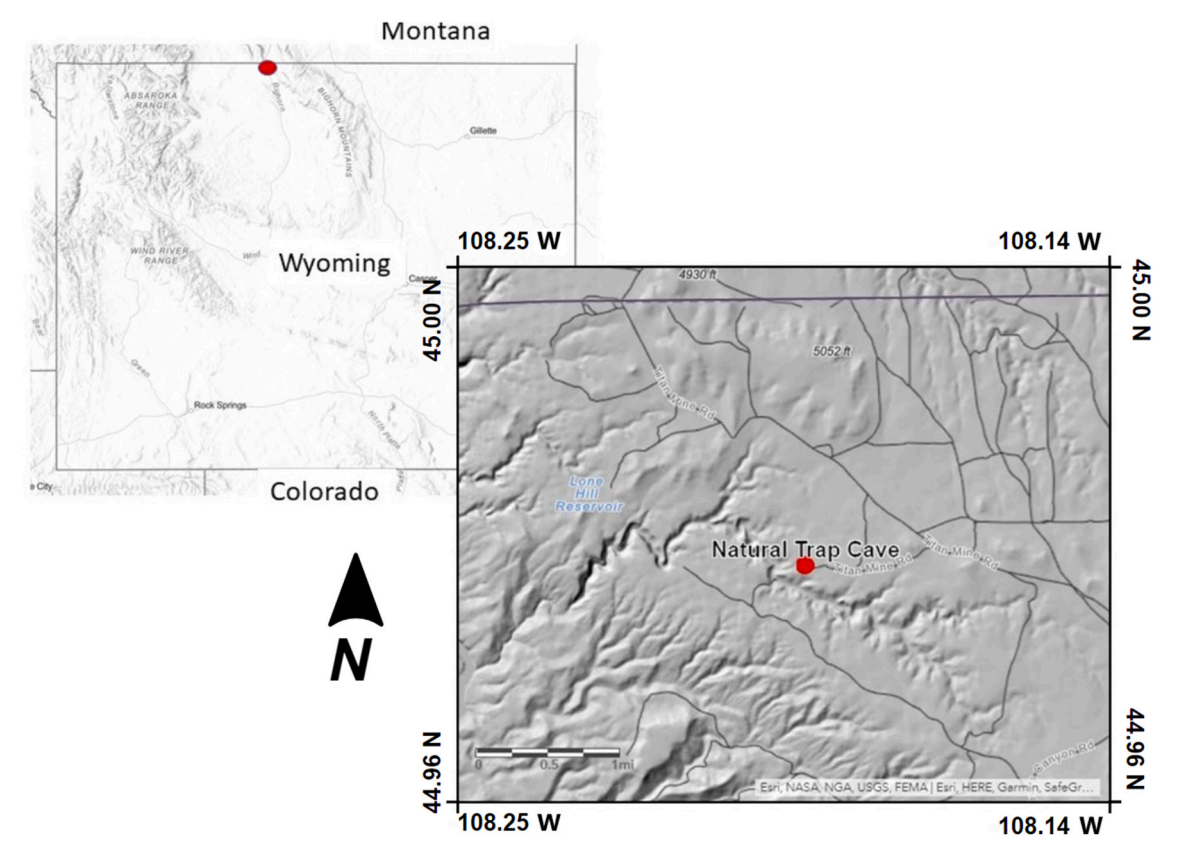


Fig. 1. Natural Trap Cave is just south of the Wyoming-Montana border, in the northern Bighorn Mountains.

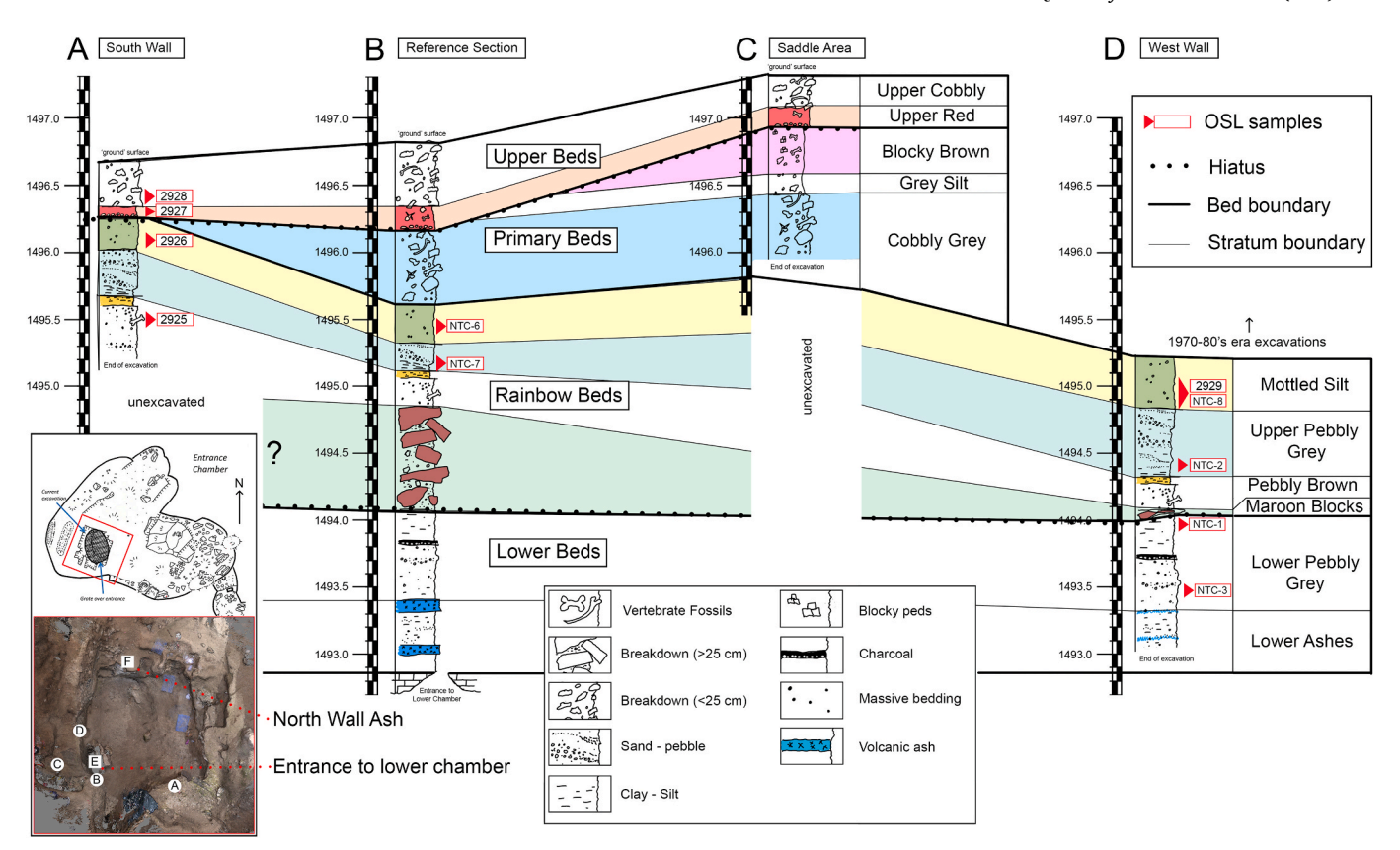


Fig. 2. NTC stratigraphy with OSL sampling locations (modified after Lovelace et al., this issue). The North Wall samples (NTC-4 and NTC-5) are not shown.

The formation of the cave and deposition of sediments within is a story of complex processes that started during the earliest Mississippian, probably Kinderhookian to Osagian, with the deposition of the Madison Formation (Peterson, 1984; McEldowney et al., 1977; Sandberg and Klapper, 1967; Peale, 1893). The Madison Formation is comprised primarily of limestones, with some named and un-named dolomitic and shale units (McEldowney et al., 1977 and references therein), and is the result of an extensive ocean transgression into the mid-continent that created an expansive tropical carbonate platform through much of the present-day Mountain West, reaching as far east as present-day Nebraska.

In the Bighorn Mountains, the Madison Formation is overlain unconformably by the Amsden Formation which is primarily composed of siliciclastic sediments (predominantly sandstones and shales) and marks a subsequent transgression by mid-continental ocean. During the time interval of ocean regression, subaerial exposure of the Madison Formation resulted in extensive karst development with characteristic subsurface hydrology including the formation of caves and sinkholes. This time frame is associated with Kaskaskia regression and karst development elsewhere in the continent (Sloss, 1963; Sando, 1988; Sonnenfeld, 1996). In turn, the Amsden Formation deposition is correlated with Absaroka sequences transgression in North America (Sloss, 1963). This led to local deposition of basal Amsden Formation clastic sand and silt with paleosols and fluvial sandstones (Garber et al., 2018) that contributed sediment to the karst platform, infilling fissures, pipes, caves and sinkholes (Sando, 1974, 1976, 1988). The Amsden Formation is thus draped over the paleokarst terrain and Amsden Formation sediments are encountered within bedrock voids and depressions in the uppermost Madison Formation units, even where the Amsden Formation has been completely eroded away (Sando, 1974, 1976).

The paleokarst played a major role in later karst development following the uplift of the Big Horn Mountains (Sando, 1974, 1976). Regional uplift and faulting created fractures and joint sets that allowed

for speleogenesis to become active within the Madison Formation again. NTC sits at the apex of an anticline influencing the hydrology and pattern of cave development. The preexisting but filled passages of the pre-Amsden Formation karst were partially exhumed, and enlarged by the renewed movement of water, and new passages formed along the fractures created during uplift of the mountains (McEldowney et al., 1977). The transition from a hypogene system, with upwelling or hydrothermal waters to an epigenetic karst, with surface openings capable of receiving direct surface contributions (e.g., water and sediment), is likely timed with development and downcutting of the Bighorn River and tributaries, and potentially occurred within the last 800 ka or less (Stock et al., 2006). For NTC, like the other caves within the drainage of the Bighorn River (i.e., Horsethief Cave, Big Horn Cavern, and Spence Cave), sediments within the cave have been derived from both allogenic (external) and autogenic (internal) sources (McEldowney et al., 1977; Stock et al., 2006).

Secondary sediments such as speleothems can reveal a paleoclimatic signal integral to their deposition. Clastic sediments within the cave can also contain an environmental signal, and this too has a history of use for illuminating paleoclimatic information. Within these studies, exploring unconsolidated clastic sediment, assessing facies, geochemical properties and lithology are critical for understanding the signals in paleo- or bioclimatic variation that might be resolved from in-cave deposits (Schwartz and Rink, 2001; Bosch and White, 2004). Clastic sediments within caves are an attractive source for paleoclimatic reconstructions because they are abundant and, once emplaced, they can remain undisturbed by bioturbation, physical erosion and other processes that would otherwise obliterate similar surface deposits (White, 2007).

Resolving the chronology of in-cave clastic units relies on the codeposition of materials useable in biostratigraphic dating, such as pollen assemblages (Panno et al., 2004) and direct dating of macrofossils, including bone or wood fragments (e.g., Driver et al., 1996; Wood et al., 2009), or tephra (Karkanas et al., 2015; Bruins et al., 2019) with fission track or argon-argon analyses. Additional avenues include absolute ages for resolving the timing of deposition with uranium-series methods applied to situ calcite (crusts on sediment surfaces) and direct dating of fine sediments with thermal or optical luminescence (Stock et al., 2006). Luminescence ages are dependent on light exposure of the sediment prior to deposition; a factor that is seemingly counterintuitive within the dark confines of a cave but has a track record of utility (Wood et al., 2009; Bellomo et al., 2011; Veres et al., 2018).

To understand the sedimentological history of clastic deposition within a cave, especially for utility with luminescence ages, a clear model of deposition is needed. This includes any ongoing effects of speleogenesis as well as an understanding of the transport mechanisms for clastic sediment into and subsequent distribution within the cave (Bull, 1981; Murphy and Lord, 2003). Sediment entrainment can be tied to broader regional geomorphic processes, such as over-bank deposits associated with flooding and channel incision of surface drainages (Panno et al., 2004), the direct or indirect contribution from glaciation (Murphy et al., 2001) or a combination of processes including aeolian and colluvial inputs via an open entrance (Stock et al., 2006).

Besides the usual "rockfall" of sediments as the collapse feature widens in the Madison Formation, most of the unconsolidated sediments are of silt and clay size, with much of this material likely coming from the Amsden Formation, introduced through the roof opening or various passages, some now choked by sediment fill. The silt size particles consist of quartz (60%), orthoclase (25%) and plagioclase (10%) plus minor amounts of hornblende, chlorite, and biotite (Albanese, 1977; Lovelace et al., 2021a, 2021b supplemental). These minerals are not usually present within the Madison limestones, but would be expected to occur in the Amsden Formation (Lageson et al., 1979) although as noted in other work in this issue, the material could also be wind-blown as eolian sediments are frequently silt sized particles.

Frost wedges, frost cracked rock fall or other periglacial features are notably absent in NTC sediments. The absence of periglacial features (frost wedges, involuted sediments, etc.) probably indicates that the cave sediments were never subjected to extreme cold and freezing for long periods of time. This does not preclude the possible presence, at times, of ice within the cave, but evidence for this condition was not apparent to Albanese (1977). It was proposed that a snow cone would build up directly under the opening into which sediments (along with snow) may have washed, slumped and mixed, displacing sediment and vertebrate remains laterally from the cone (Martin and Gilbert, 1978; Wang and Martin, 1993). However, that has been contested and largely refuted (Lovelace et al., this issue). Stratigraphic nomenclature has been somewhat confused as various authors have created schemes different from those used during the pre-Meachen excavations. This is outlined in Lovelace et al., (this issue), and we built our luminescence ages into Lovelace's unit descriptions and nomenclature.

2. Methods

2.1. New Argon/Argon data (on the feldspars in the Middle Ash)

Three ash samples were collected from fresh exposures, two from near the entrance to the lower chamber (Samples 2 and 3; 'Lower Ashes' interval of Lovelace et al., this issue), and one from the North Wall (Sample 1) which is stratigraphically higher than the Cobbly Grey unit (Fig. 2). However, there is poor stratigraphic control for Sample 1 due to slumping and mixing of backfill from previous excavations. Sanidine was isolated from the collected samples by crushing, sieving, magnetic sorting, and density separation using methylene iodide. The separates were then ultrasonically leached in a 10% (1.2 M) HCl and rinsed ultrasonically with deionized water. A subsequent leaching procedure was performed using 10% HF (2.2 M) followed by ultrasonic rinsing with deionized water, and then hand-picking under a binocular microscope. Sample 1 (upper ash on North Wall) and Sample 2 (upper ash on the West Wall) did not yield any sanidine. Sample 1 consisted of pumice and

glass shards, similar to that reported by Albanese (1977; unpublished BLM report) which can be found in [Dataset] Lovelace et al. (2021)). Sample 2 did not have sanidine, though other feldspars were present. Sanidine was isolated from the collected Sample 3, which was the middle ash.

The purified separate was wrapped in aluminum foil, placed in a 2.5 cm aluminum disk, and irradiated along with the 1.1864 Ma Alder Creek sanidine standard (Jicha et al., 2016) at the Oregon State University TRIGA reactor in the Cadmium-Lined In-Core Irradiation Tube facility for 20 min. Single crystal fusions were performed using a 60W $\rm CO_2$ laser and the gas was analyzed using a Noblesse multi-collector mass spectrometer following the procedures in Jicha et al. (2016). Due to the extremely small crystal size (30–50 μ m), the measured argon isotope signals were only about 0.5 times larger than analytical blanks. Thus, blank analyses were formed after every sample fusion to properly characterize subtle changes in the blanks. Reported ages are calculated using the decay constants of Min et al. (2000) and analytical uncertainties, including J contributions, are reported at the 95% confidence level ($\pm 2\sigma$). Atmospheric argon value used is that of Lee et al. (2006) and results are shown in Fig. 3.

2.2. Previous tephrochronology (Upper Ash)

Tephrochronology is the use of volcanic ash and pumice (tephra) as a tool for dating and correlation. The electron microprobe, the primary analytical tool for tephrochronology, is used to analyze the glass fraction of tephra for major and minor element abundances and thereby provide a chemical fingerprint which often allows ash from different eruptions to be uniquely identified. In the late 1970's, one sample from NTC and one from nearby Horsethief Cave were collected and submitted for scanning electron microscopy (SEM) and instrumental neutron activation analysis (INAA). Both sets of analyses indicated the ashes were composed of differing proportions of major and trace elements and thus that the ashes probably came from different eruptions. A least one additional sample was collected in 1992 and is in the USGS Tephrochronology database 78W18, WY0092-08, and CJ-082904 (0.11 Ma)) but exact placement in the stratigraphy remains undocumented and CJ-082904 says Natural Trap Ash but the location is given as Yellowstone National Park. Future collection and documentation are warranted.

2.3. Previous fission track Dating (Upper Ash)

Fission track dating and TL are the same family of techniques, both having radiation defects that can be exploited to return the age of burial (TL) or low-temperature thermal histories (fission track). Fission track dating is a low temperature thermochronometer, where the measured fission track age is related to the cooling of the dated rock specimen in the top 2–12 km of the Earth's upper crust. Because fission tracks are formed through geological time, those that formed first, when a rock specimen was at greater depth and at higher temperatures, are shorter than tracks formed later when the rock cooled at shallower crustal depths (Enkelmann and Jonckheere, 2021). Fission track is most often performed on apatite or zircon in rocks and glass. However, the glass ages are not considered reliable unless the glass was checked for indications of post-depositional heating that could lead to the anomalous loss through annealing of fission tracks, known as "fading" because the phenomena would lead to lower apparent ages (Naeser et al., 1981). The isothermal plateau fission track (ITPFT) dating technique applied to hydrated glass shards was developed in the late 1980s (Westgate, 1989). This technique corrected for the effects of partial track fading by heating at 150 °C for 30 days. Accurate and precise ITPFT-ages can now be obtained consistently on tephra-derived glass provided that it had experienced simple thermal histories (Alloway et al., 2013). A sample from an ash in NTC was collected in 1979 and submitted for analysis. Although the resultant date of 110 ± 10 ka was never formally published, it was used extensively as evidence of a Sangamonian age for the

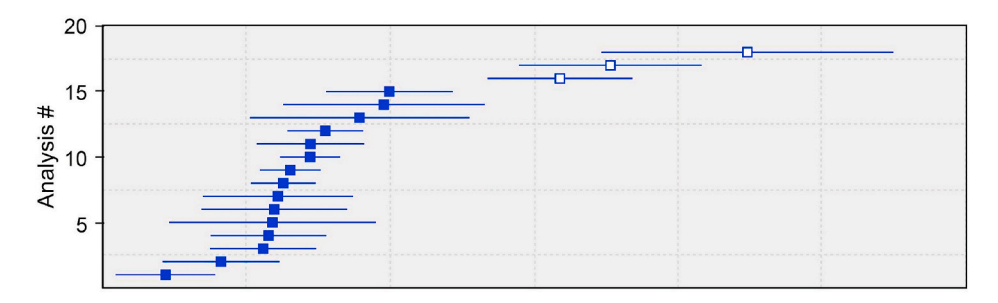


Fig. 3a. Rank order plot of single crystal fusion dates for sample of the middle ash from NTC.

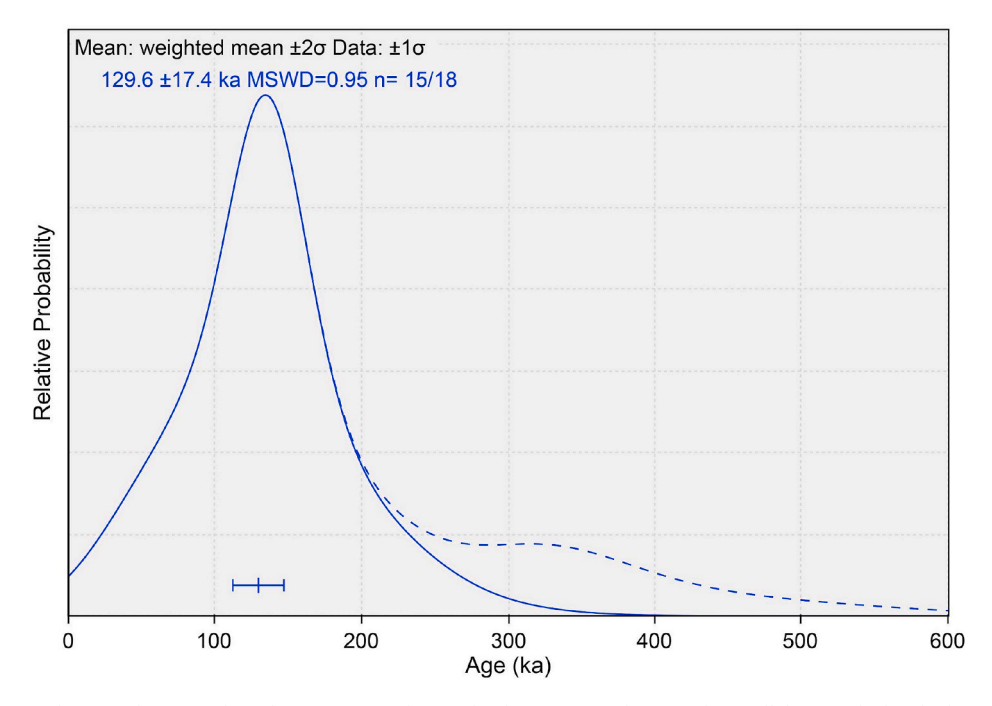


Fig. 3b. 40 Ar/ 39 Ar dates are shown with $\pm 1\sigma$ analytical uncertainties, the weighted mean age is shown with 2σ . All data is calculated relative to the 1.1864 Ma Alder Creek sanidine standard (Jicha et al., 2016). For complete 40 Ar/ 39 Ar data, see supplemental information.

stratigraphically lowest deposits within NTC. The informal 1979 report that this claim was based upon is available in the supplementary information.

2.4. Previous thermoluminescence (TL) (polymineral feldspar grains in the Upper Ash)

TL was a relatively novel technique in the 1980's whereby a luminescence age reflects the time elapsed since the last sunlight exposure (OSL) or heating event (TL). To obtain the age, two separate steps are necessary. The first step is the measurement of the equivalent dose (DE) of luminescence, or the amount of natural luminescence stored in the mineral. The second step is to measure the amount of luminescence created over time in naturally occurring radiative elements such as K, U, Th, and Rb. Luminescence is used to evaluate the trapped charge population (e.g., the amassed free electrons within the crystal lattice defects) that accumulated over time as the material was buried and sheltered from subsequent light exposure (Murray et al., 2021). The measurement in the lab mimics the natural process except that it is performed on human timescales. The samples are either heated or exposed to light under controlled conditions; in both cases trapped charges are released and combined with the resulting luminescence termed TL and OSL in the case of light exposure (Mahan and DeWitt, 2019). In TL, the temperature is increased over time and the signal is recorded versus the change in stimulation temperature. Since the 1980's, TL has expanded into a well-rounded and reliable family of luminescence chronological techniques and is performed on sediment, pottery, ash, and a wide variety of ceramics (Mahan and DeWitt, 2019). A sample from the same ash that was also fission track dated in NTC was collected in 1979 and submitted for TL analyses. The informal report is available in the supplementary information.

2.5. New luminescence (OSL on quartz and IRSL on potassium feldspar in sediments and Upper Ash)

OSL dating is the preferred technique over TL because the optical emissions from the measured grains allow for improved reliability in derived ages. The recognition that not only heating, but also exposure to sunlight resets the TL signal (Wintle and Huntley, 1979), meant that luminescence dating became applicable to the dating of light-exposed sediments. In OSL, calibrated light in the laboratory is used to stimulate natural light emission from a sample. The observation that instead of heating quartz for TL, one could expose it to intense green or blue illumination from either LED's or lasers (Huntley et al., 1985) meant practical utilization of the phenomenon of OSL for geochronology. In the late 1990's, TL dating was largely replaced by infrared stimulated luminescence (IRSL) on fine-grained feldspar silt from 4 to 11 μ m (Porat et al., 1997; Personius and Mahan, 2000; Forman et al., 2000) and by the

2000's OSL on fine-gained quartz (Wintle and Murray, 2000).

One of the main differences between TL and OSL is that during the OSL measurement there is no way of selecting only thermally stable electron traps. To overcome this problem, the sample aliquots are heated ("preheated") prior to measurement. The objective of the preheat is to empty the thermally unstable traps, with little to no impact on thermally stable traps. The quartz OSL signal is reduced to 1% of the signal after natural bleaching in full sunlight of 90 s and reaches 10% of its original value within 2 s while potassium feldspar reaches 10% loss only after 60–90 s and takes about 300 s to reduce its signal to 5% (Mahan and DeWitt, 2019). Thus, the bleaching rate of feldspars is known to be much slower and the differences in ages obtained between quartz and feldspar in the same sample can give the researcher an idea of the main transport mechanism of the grains (i.e., water vs wind).

We collected 8 samples in July 2014 and 5 samples in July 2018 following the methods described in Nelson et al. (2015) and Gray et al. (2015). Two of the 2014 samples are from the Reference Section (NTC-6 and NTC-7), 4 of the 2018 samples are from the South Wall stratigraphic section (USGS-2925, USGS-2926, USGS-2927, and USGS-2928), 3 of the 2014 samples (NTC-1, NTC-2, NTC-3) are from the West Wall section, 2 are from the ash of the North Wall Section (NTC-8 and USGS-2929), and 2 of the 2014 samples are from the North Wall, a part of the cave without a described stratigraphy (NTC-4 and NTC-5; Table 1; Fig. 2). We collected samples in one of three ways: in metal tubes, as intact blocks of sediment, or in plastic light-tight containers of varying volumes. For tube-based samples, we extracted the outer 2 cm from both ends of the tube and reserved this sample for water content determination and elemental analysis via Inductively Coupled Plasma Mass Spectrometry (ICP-MS). We then extracted the inner contents of the tube for OSL preparation and measurement.

For block samples, we spray painted the exterior of the block with black spray-paint to mark light exposed sediment. We then dismantled the block and reserved the outer 2 cm radius of the block for water content and ICP-MS derived elemental measurements. The inner contents of the block are reserved for OSL preparation. For canister collected samples, the entire sample is used for luminescence dating. Water content percent of the samples are measured and calculated using: (wet weight - dry weight)/(dry weight) for field obtained samples and again after samples are saturated with water in the laboratory to determine maximum water content of the sediment that is being dated for OSL.

To prepare the samples for OSL analyses, we treated the light-

Table 1
OSL locations and depths using the grid system set into the cave while sampling.

Location	Sample ID	Depth from floor	Grid System
South Wall:	USGS-2928	20 cm	No Grid
	USGS-2927	25 cm	No Grid
	USGS-2926	45 cm	No Grid
	USGS-2925	100 cm	No Grid
Reference Section	NTC-6	100 cm	Grid 515-520W/
			475-480N
(Mid Cave):	NTC-7	130 cm	Grid 515-520W/
			475-480N
West Wall:	NTC-2	100 cm	Grid 515-520W/
			490-495N
	NTC-1	145 cm	Grid 515-520W/
			490-495N
	NTC-3	195 cm	Grid 515-520W/
			490-495N
Undescribed	NTC-8 (upper ash)	25 cm	Grid 510-515W/
Cave			490-495N
Section (North	USGS-2929	45 cm	Grid 500-505W/
Wall)	(resample ash)		505-510N
	NTC-5	145 cm	Grid 515-520W/
			490-495N
	NTC-4	195 cm	Grid 500-505W/
			505-510N

protected sediment with a series of chemical and mechanical separations following the methods of Porat (2006). Details on the specifics of the D_E measurements, acceptance criteria, and overall sample luminescence characteristics are presented in the supplemental materials, as well as the details for the dosimetry and dose rate calculations. In general, the samples demonstrated favorable luminescence characteristics. We observed luminescence decay curves that are typical of quartz OSL with growth curves and test dose responses as observed in samples measured elsewhere from Wyoming sediments (Hanson et al., 2004; see supplemental section). We were able to compute ages using both the central age model (CAM) and minimum age model (MAM) statistical tools.

The CAM and MAM used in this report are statistical tools developed for luminescence dating (Galbraith et al., 1999; Galbraith and Roberts, 2012). They effectively solve for the dose that all grains received post-burial. The CAM assumes there is geological variability in the dose received by all grains in a population (unlike other age models). When a sample has been fully bleached prior to deposition, the CAM will isolate the true burial dose. However, fully bleached samples can be rare in some depositional environments, especially those in caves. In such cases where incomplete bleaching is expected (i.e., alluvial, fluvial, karst settings) and there is no mixing of sediments, we use the 3-parameter MAM. The MAM effectively weights the lower dose grains based on the idea that lower dosed grains are more likely to have been fully bleached prior to deposition. Note that in some cases, the CAM and MAM will produce overlapping results. This occurs when the statistical scatter of the sample is similar to the scatter expected for a well-bleached sample (20%, Cunningham and Wallinga, 2012). Both the CAM and MAM are identifying a population of luminescence characteristics most likely to represent the true depositional age. If there are overlapping results, we defer to the CAM. If they do not overlap, we generally prefer the MAM with the caveat of no mixing observed. However, the decision of which age model to prefer involves multiple factors and varies on a case-by-case basis.

3. Results

Details of the complex stratigraphy are documented in Lovelace et al., (this issue). The stratigraphy is described based on color, structure, age of sediment or organisms contained within the sediment, and fossil assemblage. It has been particularly beneficial to combine a variety of geochronological methods to cover the timeline in the cave (Fig. 4).

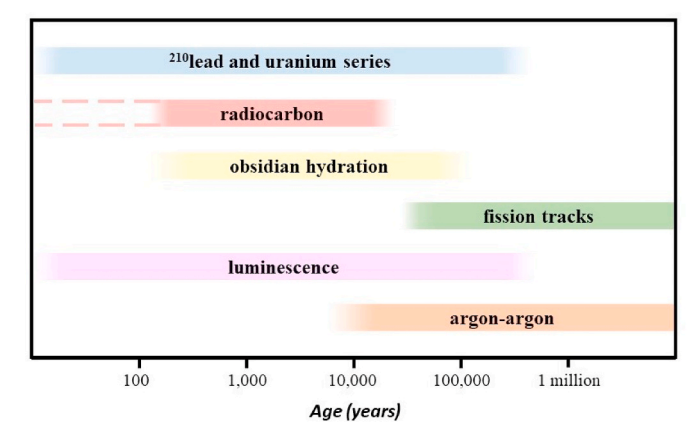


Fig. 4. Overlap of techniques used to date ash, sediment, and organic remains of NTC. Figure modified from Aitken (1988) and utilizes a log scale at the bottom.

3.1. Tephrochronology (Upper Ash), Argon Dating (Middle Ash), and obsidian hydration Dating (Upper Ash)

Currently, there are three distinct ashes denoted within the stratigraphic framework in NTC (Lovelace et al., this issue). Albanese (Albanese, 1977) was the first to note the presence of an ash in the upper stratigraphic layers, further remarking that little had been done with the ash up to that point. During the 1980 excavation, two additional ashes were found below the ash dated by Gilbert et al. (1980; unpublished 1979 report). As far as we can ascertain, at least one of the three ashes, most likely the large upper ash, was collected during work in 1978–1979 and is in the USGS Tephrochronology Database (J. Knott, California State University-Fullerton, personal communication; supplemental material) with descriptive elemental compositions. Collecting, describing, and cataloging additional samples of the lower ashes in the database would be helpful for understanding the geologic history of the NTC.

The middle ash was dated to 130 ± 17 ka by argon/argon dating and the other two ashes did not yield sufficient sanidine for an argon age. In a 1980 BLM report, Gilbert states (via personal communication) that Virginia Steen-McIntyre obtained an obsidian hydration date on the upper ash that was also dated with fission track and TL, and she obtained an age between 70 and 100 ka.

3.2. Fission track and TL (Upper Ash)

Locally, an ash from river terrace deposits along the entrance to the Bighorn Canyon was reportedly dated to 600,000 years by USGS (Larson et al., 1976; Stock et al., 2006) and found to be comparable to Pearlette type O ashes across the Great Plains (e.g., Naeser et al., 1981; Zakrzewski, 1975). Two ashes were reported from Horsethief Cave (Larson et al., 1976) and a fission track date from NTC was reported in an abstract (Gilbert, 1980a, 2018b); although no analytical methods, calculations, or standards were included. The fission track dating was conducted by John Boellstorff (a coauthor on the Gilbert, 1980a, 2018b abstract) and, later in our research, we found results that outlined the calculations and the Borchers Standard that was run alongside NTC samples (supplemental information).

Due to lack of precision documentation, it is suspected that the fission track dating determined in 1979 is almost certainly on the upper ash layer of the 3 layers that are below the sediments that we dated with luminescence. The ages (110 \pm 10 ka) contrast with the OSL ages (26–30 ka) although we note that OSL only dates the last depositional event. The upper ash layers have almost certainly been reworked; the sediments contain terrigenous fractions comprised of sub-rounded grains, potentially indicating secondary transport. Additionally, and importantly for both the TL and OSL analyses, sunlight does hit the floor of the cave where the ash was sampled, maintaining the potential for sunlight bleaching after deposition. We also note that our measured major element percentage of K does not match the 1980 Gilbert report percentage of K due to a difference in reported units (Table 2; ours is 2.02% (gamma spectrometry) and 1.75% (ICP-MS) and the 1981 report is 1.19–1.21 relative counts/second/gram for neutron activation analyses) so it is unclear whether we dated the same ash as the earlier efforts by Gilbert and collaborators.

In 1979, R. M. Rowlett analyzed samples of NTC and Horsethief Cave ashes by TL to try and determine an age for each of the ashes; these data went unpublished (Rowlett, 1980; supplemental). A calculated TL age originally reported as MATL 79-12A: $2.9.2\pm25\%$ ka, was reported for one of two ashes in Horsethief Cave (it is unknown which of the two ashes is represented by this sample). The NTC sample was reported to have a calculated TL age originally reported as MATL 79-12B: "rhyolitic tephra" $49.7\pm11.5\%$ ka (Rowlett, 1980 unpublished report), and was shown to be compositionally different from that of Horsethief Cave (Gilbert, 1980a, 2018b; unpublished results submitted in NSF annual report) indicating preservation of two different volcanic events in two different caves (see supplemental of tephrochronology reports). We

 Table 2

 Sample data used to calculate the luminescence dose rates.

Lab ID	Depth (m) ^d	Water Content ^a	K (%) ^b	U (ppm) ^b	Th (ppm) ^b	DR (Grey/ ka) ^c
Ls.	0.00	_	0.40	31.6 ±	3.1 ±	_
North			±	0.79	0.16	
Wall			0.03			
Ls. West	0.00	-	0.25	$30.9 \pm$	$2.6 \pm$	-
Wall			±	0.77	0.13	
			0.02			
Ls. East	0.00	-	0.45	42.8 ±	3.8 ±	-
Wall			\pm 0.04	1.07	0.19	
NTC-1	1.45	12 (38)	1.60	$1.99 \pm$	7.49 ±	2.42 ± 0.07
MIC-I	1.43	[25]	±	0.24	0.45	(feldspar)
		[20]	0.07	0.21	0.10	2.09 ± 0.06
			0.07			(quartz)
NTC-2	1.00	14 (14)	1.85	$2.65 \pm$	8.73 \pm	2.77 ± 0.07
		[14]	\pm	0.23	0.46	(quartz)
			0.07			_
NTC-3	1.95	12 (13)	1.01	$1.90\ \pm$	6.04 \pm	2.11 ± 0.08
		[12]	±	0.25	0.38	(feldspar)
			0.05			1.69 ± 0.06
						(quartz)
NTC-4	1.95	10 (13)	0.92	1.68 ±	5.13 ±	2.03 ± 0.06
		[12]	±	0.22	0.27	(feldspar)
NTC-5	1.45	8 (39)	0.04 0.87	$1.59 \pm$	5.81 \pm	1.33 ± 0.07
NIC-3	1.43	[24]	±	0.26	0.42	(quartz)
		[27]	0.09	0.20	0.42	(quartz)
NTC-6	1.00	8 (24)	0.86	$1.34~\pm$	$5.20 \pm$	1.36 ± 0.06
		[16]	±	0.25	0.55	(quartz)
			0.05			
NTC-7	1.30	8 (9) [8]	1.66	2.73 \pm	9.01 \pm	2.80 ± 0.07
			±	0.31	0.51	(quartz)
			0.05			
NTC-8	0.30	2 (36)	2.02	$3.55 \pm$	$11.9 \pm$	3.53 ± 0.08
(ash)		[19]	±	0.24	0.40	(feldspar)
			0.05			3.16 ± 0.06
Complee of	ove this li	no moneurod :	rith comm	a canatromo	trus thoso ho	(quartz) low by ICP-MS
USGS-	1.35	5 (33)	0.97	1.36 ±	5.2 ±	1.39 ± 0.03
2925	1.00	[19]	±	0.03	0.26	(quartz)
		[]	0.03			(4
USGS-	0.62	14 (55)	1.65	$2.05\ \pm$	9.3 \pm	2.07 ± 0.04
2926		[34]	±	0.05	0.47	(quartz)
			0.04			
USGS-	0.38	1 (39)	1.78	2.44 \pm	9.5 \pm	2.57 ± 0.05
2927		[20]	±	0.06	0.48	(quartz)
*****	0.00	10 ((0)	0.04	0.00	0.0	1 21 1 0 0 1
USGS-	0.30	13 (62)	1.67	2.03 ±	9.2 ±	1.71 ± 0.04
2928		[38]	±	0.05	0.46	(quartz)
USGS-	0.45	9 (49)	0.04 1.75	2.27 \pm	10.4 \pm	2.42 ± 0.04
2929	0.43	9 (49) [29]	1./5 ±	2.27 ± 0.06	0.52	2.42 ± 0.04 (quartz)
(ash)		[42]	0.04	0.00	0.52	(quartz) 2.79 ± 0.06
·/						(feldspar)

^a Percent water content of field sample used for age calculation, number in parentheses represents the saturated water content, square brackets show modeled water content (Nelson and Rittenour, 2015).

^b Determined by high resolution Ge gamma spectroscopy for the 2015 samples or ICP-MS for the 2018 samples. In-situ gamma spectrometry was also performed to check for U disequilibrium.

^c Calculated using the Dose Rate Age Calculator (Durcan et al., 2015).

 $^{^{\}rm d}$ Elevation is taken from the floor of the modern cave and is 1,487 m. The cave is 24.5 m deep to the "floor", elevation at top is 1,512 m. Depth is taken from cave floor elevation plus "overburden". Cosmic dose rates at bottom of the cave are $\sim\!0.05$ Gy/ka mainly due to shielding of the sediments by 20–25 m of limestone bedrock.

assume the errors on the TL dates are to 1σ as this is the standard method of reporting luminescence precision.

3.3. OSL (Sediments and upper Ash)

Water, as a transport agent, reduces the bleaching rate of luminescence in the minerals that are measured to produce the age since the most efficient wavelength of bleaching is ultraviolet spectrum (UV), which is strongly attenuated by water. Because the stimulation of crosssections of quartz and feldspar depend on different wavelength of light (Spooner, 1994; Bøtter-Jensen et al., 1994) even the qualitative effects of time-variant, simultaneous changes in spectrum and intensity are difficult to predict (Murray et al., 2012). What is known with some certainty is that quartz will bleach at a much faster rate than the feldspar when transported by water, while both are generally evenly bleached if transported by eolian processes (Mahan and DeWitt, 2019). As a mineral grain enters a cave, short transport distances (such as those that occur during sheet erosion, transport into a cave, or colluvial transport on a fault scarp) would probably dominate over the much longer transport distances (e.g., after entering a river, blowing in the wind or through hillslope transport). It is likely that the mineral bleached before it entered the cave system, due to the longer path the grain would have taken to get into the cave as opposed to a relatively short path it can take once in the cave. Although sunlight does penetrate to the floor of the cave it is of limited scope.

3.3.1. Dose rate

It is important to evaluate the rate at which luminescence builds within the grains of quartz or feldspar. The luminescence clock begins 'ticking' through isotopic decay of radioactive elements such as K, U, and Th and is called the dose rate. These elements and the associated radioactive decay come directly from the surrounding sediment. The elemental concentrations are quite different for the limestone rocks and the sediment that the fossils are encased in (Table 2). The limestone character of the bedrock ensures that any fragments of bedrock that are dissolved or finely comminuted into the cave floor sediment will contribute a very small or negligible proportion of feldspars and quartz to the sediment matrix, therefore the radioactive elemental concentrations are quite low, except for the U (Table 2; also supplemental tables). Most of the fine-grained sediments are sourced from geology at the top of the sinkhole with minor influence coming from the large blocks of limestone or paleo-cave breccia that have fallen to the cave floor.

We measured the K-, U-, and Th-concentration values from in situ 4-channel gamma field spectrometry, laboratory high-resolution gamma spectrometry, and ICP-MS; although not all samples were measured with each of these methods (Table 2; for a detailed look at the techniques used please see Mahan and Krolczyk, 2022). The results indicate general agreement among the three methods. Moreover, from the gamma spectrometry data, there appears to be no significant (for dose-rate calculations) radioactive-decay-series disequilibria (OlleyMurray and Roberts, 1997; Berger et al., 2004). For this reason, and others outlined in the Supplementary materials, we chose to calculate the dose rates using the gamma spectrometry for the 2014 samples and ICP-MS for the 2018 samples.

3.3.2. Equivalent dose

It is equally important to evaluate the amount of natural luminescence already present within the grains of quartz or feldspar. This is measured in a "dark lab" under controlled conditions and also replicated with a laboratory dose that recreates the sensitivity corrected luminescence signal produced in nature and together this process produces the D_E . D_E (Gy) divided by the dose rate (Gy/ka) returns the age (ka). We measure the quartz OSL or feldspar IRSL using the single aliquot regeneration (SAR) protocol.

The samples were run on an automated Risø TL/luminescence- DA-20 for quartz and feldspar luminescence. Data generated in this study

and unpublished reports from previous studies are included in supplementary materials in this report for reader's convenience and are available in Mahan and Krolczyk (2022). These graphs are examined by laboratory staff during measurement to check for signs of contamination by non-quartz or feldspathic minerals or for evidence of luminescence saturation. We attempted to run between 30 and 48 aliquots per sample. However, factors such as sample or machine availability can limit the number of runs performed or if laboratory staff determine that further aliquots are not necessary to calculate an age.

Overall, samples collected from NTC were amenable to luminescence dating and generally demonstrated favorable luminescence characteristics. We observed luminescence decay curves that appear to be typical of quartz OSL or feldspar IRSL with growth curves and test dose responses as observed in samples measured elsewhere in Wyoming (Hanson et al., 2004) (see plots in supplemental). We were able to compute ages using both the CAM and MAM statistical tools (Table 3; Galbraith et al., 1999). All errors are reported to 2σ in order to facilitate efforts of Bayesian Modeling.

4. Discussion

4.1. Stratigraphy

As extensively explored in other papers of this dedicated issue, large amounts of debris, animals, and sediment would often have catastrophically entered NTC punctuated by long intervals of time with incremental build-up of sediment (dust) and smaller organics (pollen). The unifying effect of a cohesive stratigraphy as outlined by Lovelace et al., (this issue) is the keystone for producing a framework and context in which to place all our chronology and data (Fig. 2). Placing the chronology into a Bayesian model allows stratigraphic relationships and ages by multiple techniques (C-14, OSL) to be combined into a self-consistent age-depth model. Combining these different datasets therefore reduces the uncertainties that would be present in each of these datasets individually. Numerous radiocarbon ages have been carefully evaluated before being placed in the model and full details should be read thoroughly in Lovelace et al., (this issue). There are also some inconsistencies with the luminescence ages (note in Fig. 2, also Lovelace et al., this issue) that are almost certainly because of partial bleached characteristics and these are highlighted in Table 2.

While luminescence age reversals in stratigraphic sequences may occur due to sampling or laboratory error, they are possible but unlikely in our study A lab error mixing the results cannot be completely discounted either but is unlikely. That said, two likely scenarios are considered to explain incompatible stratigraphic ages: the sediment was not derived from overland sources but rather from the walls of the cave at the outset or the sediment was later mixed as periodic overland water falling into the cave swirled layers around in a very localized flood scenario, plucking the sediment and bones out of recent unconsolidated layers and pulling everything towards the drain of the lower chamber. Gilbert's own report to the NSF in 1980 records an instance of "An equally interesting although less ancient find was made as a result of a heavy rainstorm. Post-cranial bones, and the anteriorly curved horn cores diagnostic of Bootherium, an extremely rare 20,000-year-old musk ox, were found when they washed from the sidewall of our excavation."

The stratigraphic layers themselves indicate that water was the primary agent in the final deposition and the luminescence ages verify this as the feldspars are not as well bleached as the quartz (Table 3). There is the presence of layered banding, gravel lenses, pronounced erosional surfaces, and the random distribution of disarticulated bones. This all indicates the action of running water either entering through the roof or through a cave passage (Albanese, 1977; Lovelace et al., this issue). The three volcanic ash layers located adjacent to the south wall of the cave could only enter via water or wind and the ash did not stay in discrete layers, as ash can be found mixed in some nearby sediments.

The floor is depressed under the cave opening but the major fossil

Table 3Sample data used to calculate luminescence ages. Ages in bold are preferred.

Lab ID	n ^a	%Over dispersion ^b	MAM D _E (Gy)	CAM D _E (Gy)	MAM Age (ka) ^c	CAM Age (ka) ^d
NTC-1 (middle)	15 (15)	24	48.7 ± 3.8	$\textbf{70.4} \pm \textbf{4.5}$	29 ± 4.6 (feld)	42 \pm 6.7 (feldspar)
	27 (29)	29	26.7 ± 2.2	58.7 ± 3.4	13 ± 1.1 (quartz)	$28 \pm 1.8 (quartz)$
NTC-2 (top)	24 (30)	34	25.2 ± 2.9	41.6 ± 3.0	9.1 ± 1.1 (quartz)	15 ± 1.2 (quartz)
NTC-3 (bottom)	15 (15)	24	54.0 ± 4.0	66.5 ± 4.2	$37 \pm 5.9 \text{ (feld)}$	46 \pm 7.2 (feldspar)
	19 (29)	30	23.1 ± 3.5	56.1 ± 4.0	14 ± 2.1 (quartz)	33 ± 2.6 (quartz)
NTC-4	7 (10)	17	37.0 ± 3.9	41.2 ± 3.1	18 ± 3.9 (feld)	20 ± 3.9 (feldspar)
NTC-5	11 (28)	31	17.2 ± 2.7	31.1 ± 3.1	13 ± 2.1 (quartz)	23 ± 2.7 (quartz)
NTC-6	17 (28)	23	29.4 ± 3.6	38.1 ± 2.3	22 ± 2.8 (quartz)	$28 \pm 2.1 (quartz)$
NTC-7	24 (33)	20	51.2 ± 3.5	60.9 ± 2.6	18 ± 1.3 (quartz)	22 ± 1.1 (quartz)
NTC-8 (ash)	5 (15)	12	112 ± 12.1	137 ± 8.1	46 ± 8.4 (feld)	56 ± 9.0 (feldspar)
	12 (30)	8	90.8 ± 4.3	90.8 ± 2.9	29 ± 1.5 (quartz)	29 ± 1.1 (quartz)
USGS-2925 (bottom)	34 (38)	33	18.1 ± 1.2	34.3 ± 1.9	13 ± 0.9 (quartz)	25 ± 1.5 (quartz)
USGS-2926	40 (40)	21	22.4 ± 1.1	30.4 ± 1.0	11 ± 0.6 (quartz)	15 ± 0.6 (quartz)
USGS-2927	44 (44)	11	19.4 ± 0.7	20.6 ± 0.4	7.6 ± 0.3 (quartz)	$8.0 \pm 0.2 (quartz)$
USGS-2928 (top)	37 (40)	22	22.0 ± 1.5	31.6 ± 1.1	13 ± 0.9 (quartz)	19 ± 0.8 (quartz)
USGS-2929 (ash)	10 (12)	14	39.1 ± 2.8	75.3 ± 4.4	14 ± 3.6 (feld)	27 ± 1.3 (feldspar)
	42 (43)	34	14.2 ± 1.0	26.8 ± 1.4	$10\pm0.7~\text{(quartz)}$	10 ± 0.7 (quartz)

^a Number of aliquots meeting acceptance criteria, parentheses indicate total number of aliquots measured.

bearing area is to the north and west of the opening and five feet upslope. Any upslope transport of material would have been difficult under normal fluvial conditions. As suggested earlier, a prevalent "snow cone" hypothesis was advanced by the 1980 team. This feature would have been capable of producing mixed sediment and periodic sheets of water through an annual snow or ice cone that built up under the opening during cooler and wetter Pleistocene surface conditions. Such a feature would have eroded or melted away after the Pleistocene, perhaps even seasonally. Present summertime conditions were recorded at 42 °F and 98% humidity within NTC (Martin and Gilbert, 1978) and other caves at higher elevations nearby (Pryor Mountains) have year-round ice. The 1980's science team hypothesized that falling animals and overland flow sediment would slide laterally some distance from the center of impact. They suggested the east-west profile along the 480N line (which is parallel to, and 1.5 m from the south wall in Fig. 2), shows virtually level strata, however Lovelace et al., (this issue) did not find that to be the case and argues against the snow cone concept suggesting instead it was a falling trajectory. Nonetheless, the E-W trend is interesting because it shows increasing optical and radiocarbon ages towards the entrance of the lower chamber.

4.2. OSL Dating of the sediments

The OSL characteristics (specifically, the observed differences in laboratory bleaching, decay curve shape and difference in the DE of different minerals within the same sample) inform us that the bulk of sediments are almost certainly transported by overland water flow; supplemented minimally by wind but then at some later date, periodically and sporadically remixed colluvially as transport wash in the cave during flood episodes. Our reasoning is informed by the stratigraphic incoherence seen in some units, such as the disarticulation of animal bones with no evidence of bioturbation, and luminescence age reversals (Fig. 5a, b, 5c; Table 3). For example, NTC-6 and NTC-7 present reversals of stratigraphic conformity with the younger age on the bottom and the older age on the top (Fig. 5a), although we note that the ages would overlap within error at one sigma. The sediment characteristics may differ significantly (elemental concentrations are not within error of each other), but this is not a definitive age reversal that requires extraordinary circumstances. The simplest explanation is that there is realistic error modeling, and these deposits are in sequence (NTC-8 and USGS-2929; Table 2) with other samples from the west wall.

OSL dates in other caves within the U.S. have tended to produce ages that are too old for a variety of reasons, primarily due to the partial



Α

Fig. 5a. Picture of the west wall; white circles indicating successful OSL sampling. Circles that are x'ed out were abandoned due to hitting large clasts as there is abundant rockfall here.

bleaching effect. Partial bleaching is the retention of the luminescence signal previously accumulated that is not zeroed during the most recent event. Sediment that originates up-slope from the surface opening that is washed into the caves was almost certainly transported during energetic fluvial events (Pérez-González et al., 1999). Because mass transport was the main mechanism into the cave, it is unlikely that all of the fine-silt-sized mineral grains would have been exposed to sufficient daylight to significantly reset the luminescence clock during transport. although there is a degree of partial bleaching seen in the differences in ages between NTC-1, NTC-3, NTC-8, and USGS-2929 quartz and feldspar pairs (Table 3; the feldspar CAM ages are double the quartz CAM ages indicating feldspar did not have time to reset), these young ages indicate complete bleaching in the quartz and a large variable degree of bleaching in the feldspar if the MAM ages are compared to the quartz CAM ages.

Generally, in situations where the sediment shows partial bleaching bias (a positive or larger value skew in D_E), we strongly suspect either a short transport path or a massive sediment load (such as a flood) as well as the possible event of being washed out of shallow deposits on the cave

^b Defined as the statistical dispersion beyond what would be expected for a perfectly bleached sample.

 $^{^{}m c}$ Determined using the function calc CentralDose from the R-Luminescence package. Uncertainty is 2 σ .

 $^{^{\}rm d}$ Determined using the function calc_MinDose from the R-Luminescence package. Uncertainty is 2 σ



В

Fig. 5b. Picture of the southern portion of the west wall with white circles indicating successful OSL sampling. Circles with X's are unsuccessful attempts.

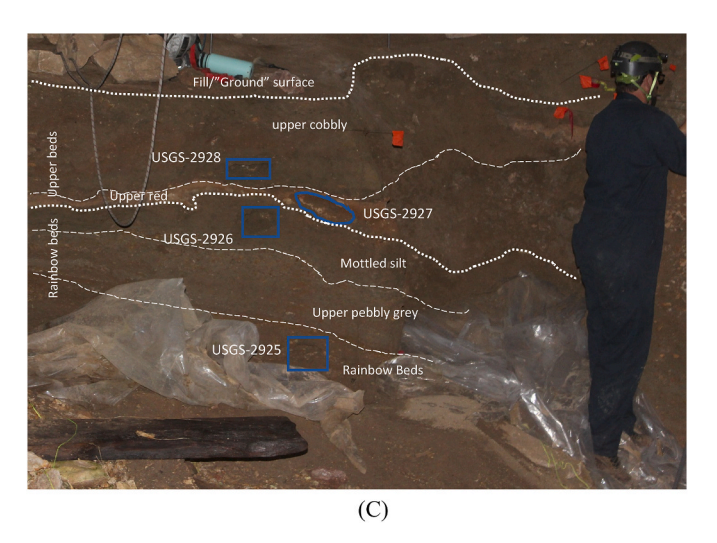


Fig. 5c. Picture of the south wall. Shown are the locations of the 2018 samples (in blue shapes) in relation to the stratigraphy of Lovelace et al. (this issue). The unconformable contact between the upper and Rainbow Beds is denoted with the dotted line, as is the "ground" surface of the section. The lighter dashed lines are the contacts of named sub-beds (Fig. 6). Person is \sim 1.6 m tall.

floor and re-exposed after a periodic flood. Use of the MAM on the measured D_E s helps to negate the partial bleaching bias, although the MAM is not ideally suited for a limited number of D_E estimates (Galbraith and Roberts, 2012) or multi grain measurements (Arnold and Roberts, 2009). However, we have no other widely used, universally acceptable, and extensively tested means of conveying a graphical representation of D_E data. The best evaluation of the age models used can be seen in the comparison between the MAM and CAM ages (Table 3).

Cave sediments are complex and erratic; sometimes the sediment being dated is introduced from the outside after being well bleached (Wood et al., 2009), sometimes it is mixed after introduction from the outside and mixed with previously laid layers (Munroe et al., 2016 Arnold et al., 2014; Demuro et al., 2019) and sometimes it is sediment that is sourced from cave walls or deep within other cave passages without much solar resetting (Driscoll et al., 2012). It is our opinion, based on luminescence bleaching rates between quartz and feldspar minerals, low overdispersion in the $D_{\rm E}$, and age, that most of the sediments were bleached of previous signals before they came into the cave

or were bleached very shortly after entering the cave. There are simply no large alluvial fans or fluvial streambed features to provide sediment other than local thin layers of sediment that would have been zeroed at the surface although we acknowledge that such features could have been there when the landscape was entering, exiting, or at full glacial conditions. There are currently no soil surveys near NTC, but this assumption could be tested in the future by digging some shallow soil pits near the surface of the cave.

It is not uncommon for there to be variance in luminescence ages for a single depositional unit as is evidenced by the scatter in the luminescence signal (Table 3, overdispersion column). The overdispersion of the D_E distribution represents the "spread" in the distribution that remains after all measurement errors, specific to each aliquot (also known as the "within-aliquot variation") have been taken into account (Galbraith and Roberts, 2012). If the sediments were adequately bleached upon entry into the cave why are there stratigraphic reversals and odd outliers in the quartz OSL that made us hesitate to use them in the MAM model? A good example is NTC-1. Of the acceptable 27 aliquots, 2 were around 20 and 24 Gy while the vast majority were somewhere between 40 and 85 Gy. There was no overlap between the \sim 22 Gy aliquots and the rest of the aliquots. Aliquot size was between 2 mm and 3 mm. Because MAM is weighted to the lower D_F based on the assumption of incomplete bleaching, we had to rethink what these results might be derived from if not incomplete bleaching. Three options are valid: 1) previous work in the cave exposed some of our sampling sites to artificial lighting from the excavations in the 1970's and 1980's, 2) there was post-depositional mixing of layers resulting in some incorporation of younger/older grains (we note this will not favor quartz over feldspar), or 3) some of the quartz grains are responding to other unknown phenomena (i.e., mineral contamination in a chert) and therefore underestimating the true D_E (Lawson et al., 2015). The MAM provides a means for effective age modelling of caves regardless of the degree of bleaching (Galbraith et al., 1999; Galbraith and Roberts, 2012) and the bootstrapped version of the model (Cunningham and Wallinga, 2012) has been shown to provide robust results for small aliquots of both well-bleached and heterogeneously bleached quartz (Chamberlain et al., 2019) although we chose not to apply more filters or bootstraps to a model than necessary since we have some outliers at the low end of the distribution. If we assume all of these conditions prevailed at one time or another, we are left with the conservative notion of using only the CAM values for the quartz OSL and the MAM values for the feldspar. Therefore, based on these conservative assummptions, preferred ages are highlighted in Table 3.

If the mixing was post-depositional, it was not catastrophic or particularly chaotic. It appears from the sediment data that there were preferred pathways of mixing and, perhaps a more likely scenario, that a slower "oozing" mixed saturated sediment rather than whole-sale rearrangement. Sediment could also have been added from other passages, although we admit this is not supported by the luminescence data. One of the most stratigraphically consistent exposures is the grouping of NTC-2, NTC-1 and NTC-3 (Fig. 2, Lovelace et al., this issue, Fig, 12). The elemental concentrations are consistent as well, even though there must be also interspersed ash in the sediments just like it is for NTC-7.

Most of the ages are in stratigraphic order and the luminescence data is quite robust (Fig. 5b; Table 3). The luminescence ages, particularly along the south wall, show stratigraphic order except for the topmost sample. USGS-2925, the bottom sample in the Pebbly Brown silt of the Rainbow Beds (Fig. 2, Table 3) is 25 ka. USGS-2926 in the upper Mottled Silt is 15 ka. At the stratigraphic unconformity of reddened sediment, USGS-2927 is 8 ka which represents a substantial amount of missing time. This missing time is discussed in some detail in Lovelace et al., (this issue) as it also occurs in the radiocarbon dates (Figs. 5c and 6, Table 3). The topmost sample, USGS-2928, is 19 ka which is so much older that the most reasonable explanation is either because it represents fill from earlier excavations, or the luminescence signal is affected by partial bleaching in these sediments, making their depositional age appear older.

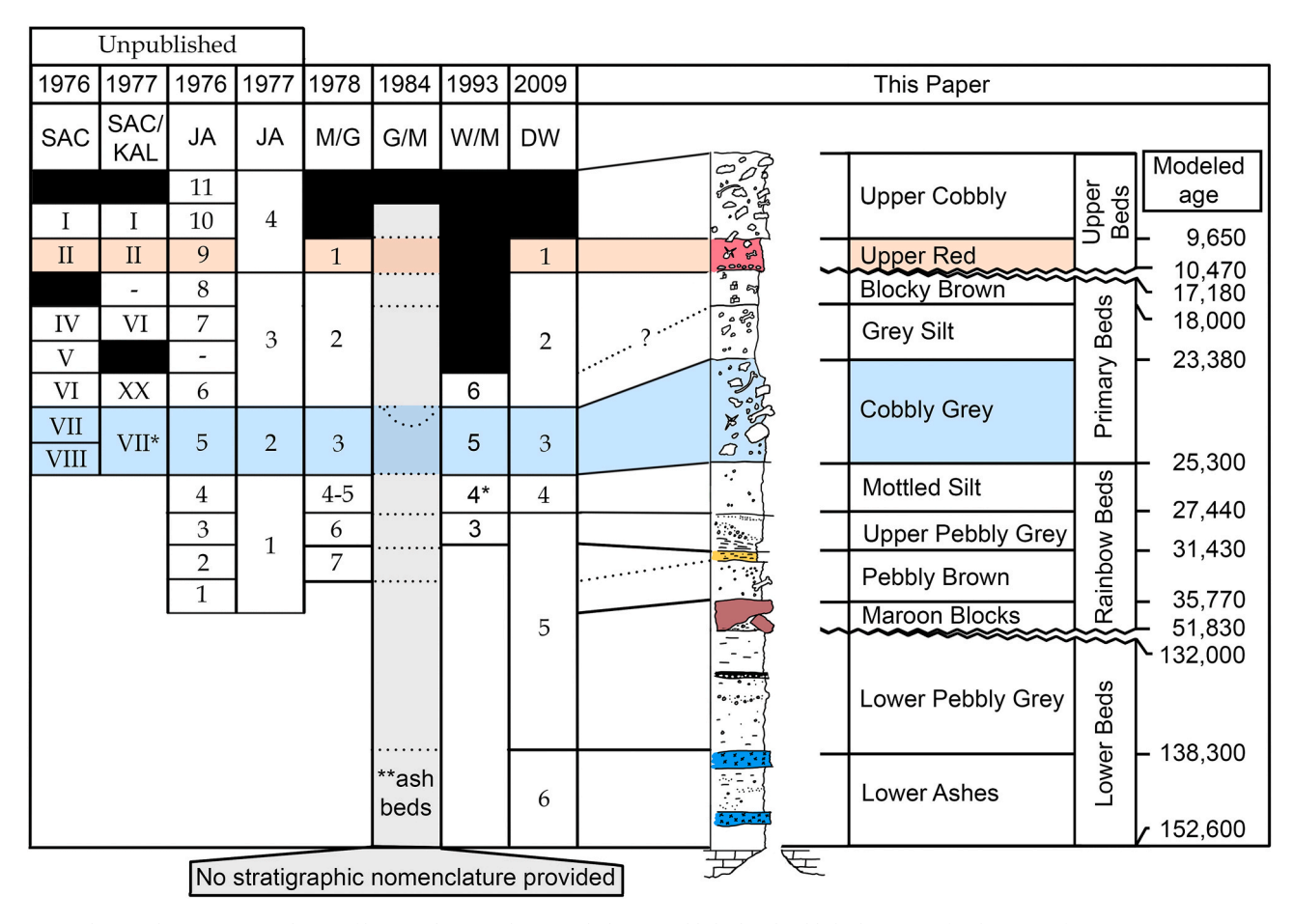


Fig. 6. (Lovelace et al. Fig, 12). Correlation of historical nomenclature including unpublished and published accounts for the years of 1976, 1977, 1978, 1984, 1993 and 2009. The various authors and their unit numbering schemes are: SAC = S. A. Chomko, SAC/KAL = S.A. Chomko and K.A. Lippencott, JA = John Albanese (1977 Unpublished Report), M/G = Martin and Gilbert (also switched as G/M for primary authorship), W/M = Wang and Martin, DW = D. Williams. These authors and units are discussed elsewhere. The Upper Red (highlighted with light red correlation) and the Cobbly Grey (highlighted with light blue correlation) share commonalities across multiple publications. **Inferred position of ashes from Gilbert and Martin (1984). (For interpretation of the references to color in this figure legend, the reader is referred to the Web version of this article.)

4.3. Tephrochronology and age of the ashes

There are three ashes present in the cave but only one of them has been previously sampled, detailed for elemental compositions or entered into the USGS Tephrochronology Database. Future work will focus on fleshing out the detail for the three ashes as to age, mineralogy, and tephrochronology unit. The upper most ash was dated at 130 \pm 17 ka using argon/argon dating on sanidine.

Schmitt et al. (this issue) demonstrate a^{230} Th/ 238 U age of 111 ± 8 ka for their North Wall Ash (the upper ash) from three spots on a single zircon; their sample was collected near our OSL samples NTC-8 and USGS 2929 (29 \pm 1.1 ka (quartz) CAM and 27 \pm 1.3 ka (feldspar) CAM; Table 1, Table 3). Gilbert states in his 1980 NSF report that the uppermost volcanic ash was dated using fission track dating, obsidian hydration dating, and TL although Gilbert notes the actual ash was just below all bone beds in the east wall at a depth of 10' (grid 490N, 510W (Table 1); Lovelace personal communication, Gilbert, 1980a, 2018bNSF report in supplemental) The lower two ashes are preserved in the entrance to the lower chamber, near OSL samples NTC-1, -2, and -3. The Schmitt et al. (this issue) date is nearly identical to the fission track date of Gilbert's 'upper ash' of 110 \pm 10 ka. In contrast, the TL age is 49.7 \pm 5.72 ka with an effective range between 55.4 and 44.0 ka based on calendar years. The ages of these two methods do not overlap and do not appear to support each other. Gilbert et al., accepted the fission track age and rejected the TL age on the basis of presumed high background radiation in the cave sediments. The TL method was thought to be too experimental while the fission track age agreed with an obsidian hydration age range of $70{\text -}100~{\rm ka}.$

USGS gamma spectrometry survey of the cave in 2018 using a scintillation detector, was conducted to pinpoint any substantial background radiation. We were unable to verify the "high background radiation" that would have rendered the TL age spurious. It is true that some layers of the limestone of the cave show elevated U/Th content (see the ICP-MS results in Table 2), and there are some secondary mineral deposits, in the form of precipitated U-rich calcite speleothems, as evidenced by the history of uranium mining in the area near NTC. The unconsolidated sediments, however, are predominately allogenic, as is the tephra recovered from inside the cave, and do not show an anomalous elevation in radiation contributions, although the recorded radon levels are rather high in the cave atmosphere (Table 2).

Why do the fission track and obsidian hydration dating appear more reliable than the TL? What should we believe based on the stratigraphy and radiocarbon dating? What are the luminescence measurements really telling us about transport and mixing that the other techniques do not? As explained earlier in the methods section, fission-track dating and TL are related techniques, and both rely on physical damage to the crystal lattice caused by external radiation. We do not know what mineral the fission track ages were obtained on when it was dated by J. Boellstorff of the University of Nebraska (the most common minerals are apatite, zircon, glass, and sometimes sphene; Supplemental 1980 Gilbert report). Since fission-track dating for young material relies on minerals with high amounts of uranium concentrations, zircon or apatite would

have been preferred but the likely candidate is glass (based on his other published papers). We know the TL was obtained on potassium rich feldspars (sanidine?) or feldspar inclusions in the glass. In both cases, to produce an age, the researcher needs to determine the U concentration (fission track does this by comparing neutron fission of ²³⁵U and TL does this by exposing the mineral to controlled heating and reading the resulting stream of photons).

Fission track is most commonly used to produce temperature data and not depositional age and it is used to date glass from 1 Ma to 2 Ga. Fission track is at its best when burial history is simple and when providing eruption temperature and provenance information of the material. TL provides the best ages when the material has been adequately zeroed by sunlight or intense heat before burial, burial history is simple, and the geologic rate of the surrounding sediment has been accurately estimated. In the absence of a detailed comparison of each sample's experimental results and a dearth of historical context, we theorize that the TL ages are just as reliable as the fission track ages, perhaps more so if we consider that the luminescence technique is probably not dating the time of formation of the ash but rather the last time it was deposited (or re-worked; see Lovelace this volume, his Fig, 8 for evidence of fluvial deposition and sorting of the ash).

Dating of the north wall upper volcanic ash by several methods establishes that is anywhere from 130 ± 17 ka (argon dating) 110 ± 10 ka (fission track) and $70{\text -}100$ ka (obsidian hydration dating by Gilbert), and two ages of $^{230}\text{Th}/^{238}\text{U}$ age of 110 ± 8 ka and 138 ± 9 ka (Schmitt et al., this issue). The upper ash of Gilbert was quite likely reworked (or at least re-exposed to sunlight) sometime around 48 ± 6 ka (TL), and the equivalent North Wall Ash shows similar evidence of reworking with an age of 26–30 ka (OSL). It is interesting to note that the 46 ± 8 ka shows up again in the feldspar IRSL age (Table 3). Since no other method is dependent on light exposure as is luminescence, the inference is that the ash has been moved within the cave during daylight by running water and redeposited in order for the younger ages to be recorded in the luminescence. The location of the ash is consistent with earlier excavations and possible exposure to sunlight.

4.4. Overall and future work

At NTC, luminescence has been helpful in defining the models of age in conjunction with the vast abundance of radiocarbon data (Fig. 6) as well as indicating the dominant form of sediment transport into the cave. Luminescence ages have occasionally been somewhat inconsistent with the stratigraphic layers (notably NTC-6 and NTC-7; Table 3), which has led to the speculation that some of the layers may have been mixed during large overland flow events. There is little evidence of hyper concentrated or debris flows, or other mass movement associated with catastrophic deposition. There are laminations and other minor bedding structures in most of the stratigraphy that suggest typical sedimentation processes. Our theories for the reversal of NTC-6 and NTC-7 ages are that there is either mixing of the sediment in a slow ooze like way, an unrecognized unconformity, a mislabel, or a lab mix-up. Evidence from Gilbert's report (1980) that major erosion and exposure happened after a rain storm is interesting, but this would have occurred with an artificial slope created during excavation, as opposed to the natural depositional slope. There undoubtedly was major erosion and translocation of material at certain points in the caves history but the details remain to be documented.

Some of the most exciting items that can be reevaluated in a new light is the data from an early TL experiment, fission track dating, and tephrochronology analyses. These data indicate that Gilbert's 'upper ash' and our 'upper ash' (North Wall Ash of Schmitt et al., this issue) represent volcaniclastic material originally deposited between about 100 and 140 ka and almost certainly reworked sometime around 50-30 ka into their positions where they were sampled. This may further explain the absence of the 110 ka 'upper ash' in the reference section where the two lower ashes (129/138 ka) are exposed; it may have been

completely removed from this location, or potentially at the modeled boundary (Lovelace et al., this issue) near 50 ka. The North Wall stratigraphy is going to be very important to work out. There may be multiple reworking of the 110 ka ash – which, given the nature of the cave, may be the most logical reason. It also helps to consider the two chronologies that the TL and fission track tell and why they give completely different ages.

Clearly, further research into both sediments in the cave as well as sediment above the cave surface is needed to answer some outstanding questions on the stratigraphy as well as new questions that have cropped up during this study. In 2021, a NTC field crew conducted a preliminary examination of the lower cave below the main cave and revealed that the sediment has been chaotically mixed to such an extent that virtually no luminescence ages will be useful. The sediment is a mixture of very fine particles resulting in a soupy texture that is mixed and unevenly distributed. There is no expectation of being able to extract useful stratigraphic context or chronology in this chamber (Mel Reusche, Uninversity of Wisconsin, personal communication, 2021).

This then leaves the surrounding ground above the cave as the only useful resource to defining sediment transport into and within the cave. Research indicates no previous geomorphic or soils study on the surrounding area within the small plateau that the cave is formed beneath. Careful excavation of several small soil pits with a descriptive study of the soils and sediments would provide background into the length of the transport path, dominant size of particles being washed into the cave, and source geology. It would also aid in understanding the timing and mechanisms of sediment emplacement on the slopes of the plateau through the application of luminescence characteristics. Samples could be taken for luminescence dating that would indicate the surface bleaching processes and rates. A description of any soils that are preserved would help in evaluating the residence of time of sediment atop the largely bare bedrock surface.

5. Conclusions

NTC is truly a unique preservation site of not only Pleistocene fossils but for the processes that shape, modify, and in-fill karst systems. Several decades of study has led to a developed and uniform stratigraphic framework, a cohesive and explainable chronology based on multiple methods for many different types of samples, and a clear vision for future endeavors. Measured luminescence characteristics imply that the dominant source of sediments to the cave floor was through overland fluvial flow with minor amounts of eolian additions. Most of the sediment originates outside of the Madison Formation and is almost certainly sourced from the surface exposures of the Amsden Formation as indicated by the elemental concentrations. These sediments are then carried into the cave through overland flow.

Luminescence ages on quartz rich sediment show it is well bleached at deposition and suitable for OSL dating but the feldspar shows evidence of not being totally zeroed before deposition. This, again, strongly implies the sediment was deposited by running water since wind dispersion completely bleaches both minerals. There are also some stratigraphic inconsistencies (reversals in luminescence ages) that point to post-depositional mixing of sediment, most likely by later flood waters that unevenly mixed loose sediment on the cave floor and pulled fine-grained sediment towards a lower chamber that has not been dated.

All luminescence ages point to a young (9–40 ka) fossil assemblage at the top of the first 2 m of sediment and the ages generally align with radiocarbon, including a gap in luminescence ages between the transition of the Pleistocene to the Holocene. There are three stratigraphic successions of ages of the upper ash in the sediments. two are dated with U/Pb to 138 ± 9 ka, argon at 130 ± 17 ka (middle ash), fission track at 110 ± 10 ka (upper ash), and obsidian hydration at 70–100 ka (also the upper ash). The same upper ash is dated at 48 ± 6 ka (TL), and 26–30 ka (OSL; 2 ages) which strongly implies the upper ash has been reworked and re-exposed to sunlight after the initial deposition. Sediment

deposition was almost certainly not continuous but largely sourced from outside the cave; these details are the subject of future studies.

Author contributions

Conceptualization, Shannon Mahan, Jack Wood, David Lovelace, Julie Meachen; Methodology, Shannon Mahan and Jack Wood; Investigation, all authors; Formal analysis, Shannon Mahan, Jack Wood, David Lovelace, Julie Meachen; Data Curation, Shannon Mahan and David Lovelace; Resources (Geochronology), Shannon Mahan and David Lovelace; Resources (cave safety), Juan Laden; Visualization and Writing (Original draft), Shannon Mahan, Jack Wood, David Lovelace, and Julie Meachen; Writing (Review and editing), all authors; Funding acquisition, Shannon Mahan and Julie Meachen.

Data availability

Datasets related to this article can be found at (Mahan and Krolczyk, 2022))an open-source online data repository hosted at USGS Science-Base. All historical documents of previous research can be found in [Dataset] Lovelace, David; Redman, Cory, Sims, Megan (2021), "Natural Trap Cave: Historical Documents, photos, and related datasets.", Mendeley Data, V1, doi: 10.17632/f8frrskzpz.1

Declaration of competing interest

The authors declare that they have no known competing financial interests or personal relationships that could have appeared to influence the work reported in this paper.

Acknowledgements

A sincere and grateful thank you goes to our co-author Juan Laden for support in getting into and, more importantly, getting out of the cave. His knowledge of other local caves in the area proved invaluable in assessing history of the stratigraphy. This project was made possible by the Wyoming Bureau of Land Management permit number PA-13-WY-207 to JAM, and we would like to thank B. Breithaupt and G. Hurley of the BLM Wyoming office for their assistance. Thanks also to Dr. Brian Jicha (WisAr Geochronology Labs) from DL. This project was funded under the Climate Research Program of the US Geological Survey (SAM). It was also partially funded by an NSF grant to JAM (EAR SGP 1425059) and JAM's NGS grant 9479-14. Reviews of previous versions of this paper by Jeff Honke, Nathan Brown, and Corey Redman helped provide structure and rigor to this version. Any use of trade, firm, or product names is for descriptive purposes only and does not imply endorsement by the U.S. Government.

Appendix A. Supplementary data

Supplementary data to this article can be found online at https://doi.org/10.1016/j.quaint.2022.01.005.

References

- Albanese, 1977. Unpublished. doi: 10.17632/f8frrskzpz.1. Available in [Dataset] Lovelace, David; Redman, Cory; Sims, Megan, Natural Trap Cave: Historical Documents, photos, and related datasets., V1 Mendeley Data. In this issue.
- Alloway, B.V., Lowe, D.J., Larsen, G., Shane, P.A.R., Westgate, J.A., 2013. Tephrochronology. In: Elias, S.A. (Ed.), The Encyclopedia of Quaternary Science, 4, pp. 277–304. https://www.sciencedirect.com/referencework/9780444536426/encyclopedia-of-quaternary-science.
- Arnold, L.J., Roberts, R.G., 2009. Stochastic modelling of multi-grain equivalent dose (De) distributions: implications for OSL dating of sediment mixtures. Quat.
- Arnold, L.J., Demuro, M., Parés, J.M., Arsuaga, J.L., Aranburu, A., Bermúdez de Castro, J.M., Carbonell, E., 2014. Luminescence dating and palaeomagnetic age constraint on hominins from Sima de los Huesos, Atapuerca, Spain. J. Hum. Evol. 67, 85–107. https://doi.org/10.1016/j.jhevol.2013.12.001.

- Bellomo, L., Hanson, P.R., Jennings, C.E., Calvin Jr., A.E., 2011. Optically stimulated luminescence (OSL) dating of glacial sediment in Crystal Cave, WI. Geol. Soc. Am. Abstracts Prog. 43 (2), 450.
- Benson, L., Madole, R., Landis, G., Gosse, J., 2005. New data for late Pleistocene Pinedale alpine glaciation in Southwestern Colorado. Quat. Sci. Rev. 24, 49–65.
- Berger, G., Melles, M., Banerjee, D., Murray, A.S., Raab, A., 2004. Luminescence chronology of non-glacial sediments in Changeable Lake, Russian High Arctic, and implications for limited Eurasian ice-sheet extent during the LGM. J. Quat. Sci. 19 (5). 513–523.
- Bøtter-Jensen, L., Poolton, N.R.J., Willumsen, F., Christiansen, H., 1994. A compact design for monochromatic OSL measurements in the wavelength range 380-1020 nm. Radiat. Meas. 23, 519-522.
- Bosch, R.F., White, William B., 2004. Lithifacies and transport of clastic sediments in karstic aquifer. In: Sasowsky, I.D., Mylroie, John E. (Eds.), Studies of Cave Sediments: Physical and Chemical Records of Paleoclimate. Kluwer Academic/Plenum, New York, pp. 1–22.
- Bruins, Hendrik J., Keller, Joerg, Kluegel, Andreas, Kisch, Hanan J., Katra, Itzhak, van der Plicht, Johannes, 2019. Tephra in caves; distal deposits of the Minoan Santorini eruption and the Campanian super-eruption. Quat. Int. 499 (Part B), 135–147.
- Bull, P.A., 1981. Some fine-grained sedimentation phenomena in caves. Earth Surf. Process. Landforms 6, 11–22.
- Chamberlain, E.L., Goodbred, S.L., Hale, R., Steckler, M.S., Wallinga, J., Wilson, C., 2019. Integrating geochronologic and instrumental approaches across the Bengal Basin. Earth Surf. Process. 45 (91), 56–74. https://doi.org/10.1002/esp.4687.
- Cunningham, A.C., Wallinga, J., 2012. Realizing the potential of fluvial archives using robust OSL chronologies. Quat. Geochronol. 12, 98–106.
- Demuro, M., Arnold, L.J., Aranburu, A., Sala, N., Arsuaga, J.L., 2019. New bracketing luminescence ages constrain the Sima de los Huesos hominin fossils (Atapuerca, Spain) to MIS 12. J. Hum. Evol. 131, 76–95. https://doi.org/10.1016/j. jhevol.2018.12.003.
- Driver, J., Handly, M., Fladmark, K., Nelson, D., Sullivan, G., Preston, R., 1996.
 Stratigraphy, radiocarbon dating, and culture history of Charlie lake cave, British Columbia. Arctic 49 (3), 265–277.
- Driscoll, D.G., O'Connor, J.E., Harden, T.M., 2012. Results of paleoflood investigations for spring, rapid, Box Elder, and Elk Creeks, black Hills, western south Dakota. In: South Dakota Academy of Science Proceedings, 91, pp. 49–67.
- Durcan, J.A., King, G.E., Duller, G.A.T., 2015. DRAC: dose rate and age calculator for trapped charge dating. Quat. Geochronol. 28, 54–61.
- Dyke, A.S., 2003. An outline of North American deglaciation with emphasis on central and northern Canada. In: Ehlers, J. (Ed.), Extent and Chronology of Quaternary Glaciation. Elsevier.
- Enkelmann, E., Jonckheere, R., 2021. Fission track dating. In: Alderton, D., Elias, S. (Eds.), Encyclopedia of Geology, second ed. Academic Press, pp. 116–130.
- Forman, S.L., Pierson, J., Lepper, K., 2000. Luminescence geochronology. In: Noller, J.S., Sowers, J.M., Lettis, W.R. (Eds.), Quaternary Geochronology: Methods and Applications. American Geophysical Union, Washington, DC.
- Galbraith, R.F., Roberts, R.G., Laslett, G.M., Yoshida, H., Olley, J.M., 1999. Optical dating of single and multiple grains of quartz from Jinmium rock shelter, northern Australia: Part I, experimental design and statistical models. Archaeometry 41 (2), 339–364
- Galbraith, R.F., Roberts, R.G., 2012. Statistical aspects of equivalent dose and error calculation and display in OSL dating: an overview and some recommendations. Quat. Geochronol. 11, 1–27.
- Garber L, K, Malone H, D, Craddock P, J, Zahm, C., 2018. Detrital Zircon U-Pb Geochronology and Provenance of the basal Amsden Formation, Bighorn Mountains. Wyoming Geological Association 72nd Annual Field Conference Guidebook 120–129.
- Gilbert, et al., 1980a. NSF Report.
- Gilbert, et al., 1980b. BLM Report.
- Gilbert, B.M., Martin, L.D., 1984. Late Pleistocene fossils of natural trap cave, Wyoming, and the climatic model of extinction. In: Martin, P.S., Klein, R.G. (Eds.), Quaternary Extinctions: A Prehistoric Revolution. University of Arizona Press, Tucson, pp. 138–147.
- Gray, H., Nelson, M., Johnson, J., Rittenour, T., Feathers, J., Mahan, S., 2015. User guide for luminescence sampling in archaeological and geological contexts. Adv. Archaeol. Pract. 3.
- Hanson R., P., Mason A., J., Goble J., R., 2004. Episodic late Quaternary slope wash deposition as recorded in colluvial aprons, southeastern Wyoming. Quaternary Science Reviews 23, 1835–1846.
- Huntley, D.J., Godfrey-Smith, D.I., Thewalt, M.L.W., 1985. Optical dating of sediments. Nature 313, 105–107.
- Jicha, B.R., Singer, B.S., Sobol, P., 2016. Re-evaluation of the ages of ⁴⁰Ar/³⁹Ar sanidine standards and super eruptions in the western U.S. using a Noblesse multi-collector mass spectrometer. Chem. Geol. 431, 54–66. https://doi.org/10.1016/j. chemgeo.2016.03.024.
- Karkanas, Panagiotis, White, Dustin, Lane, Christine S., Stringer, Chris, Davies, William, Cullen, Victoria L., Smith, Victoria C., Ntinou, Maria, Tsartsidou, Georgia, Kyparissi-Apostolika, Nina, 2015. Tephra correlations and climatic events between the MIS6/5 transition and the beginning of MIS3 in Theopetra Cave, central Greece. Quat. Sci. Rev. 118, 170–181.
- Larson, T.K., Zeimens, G.M., Walker, D.N., Frost, N., Simpson, C., 1976. An archaeological reconnaissance of the little mountain area, Big horn county, Wyoming. Wyoming Archaeol. 19 (3–4), 7–67.
- Lawson, M.J., Daniels, J.M., Rhodes, E.J., 2015. Assessing Optically Stimulated Luminescence (OSL) signal contamination within small aliquots and single grain measurements utilizing the composition test. Quat. Int. 362, 34–41.

- Lee, J.-Y., Marti, K., Severinghaus, J.P., Kawamura, K., Yoo, H.-S., Lee, J.B., Kim, J.S., 2006. A redetermination of the isotopic abundance of atmospheric Ar. Geochem. Cosmochim. Acta 70, 4507–4512.
- Lageson, D.R., Maughan, E.K., Sando, W.J., 1979. Wyoming. In: The Mississippian and Pennsylvanian (Carboniferous) Systems in the United States: U.S. Geological Survey Professional Paper, 1110-U, p. 46.
- Lovelace, D.M., Redman, C.M., Sims, M., 2021a. This volume.
- Lovelace, D.M., Redman, C.M., Sims, M., 2021b. Natural trap cave: historical documents, photos, and related datasets. Mendeley Data 1. https://doi.org/10.17632/ f8frrskzpz.1.
- Mahan, S.A., DeWitt, R.L., 2019. In: Bateman, M. (Ed.), Chapter 1 in Handbook of Luminescence Dating. Whittles Publishing, p. 427.
- Mahan, S.A., Hanson, P.R., Mead, J., Holen, S., Wilkins, J., 2022. The Mammoth Site at Hot Springs, South Dakota: use of OSL dating to calibrate the sinkhole time machine. Quat. Geochronol. (in press). In preparation.
- Mahan A, S, Krolczyk T, E, . Data Release for Luminescence: Luminescence data for Natural Trap Cave, Wyoming: U.S. Geological Survey data release. https://www.sciencebase.gov/catalog/item/6148c830d34e0df5fb96b64b. U.S. Geological Survey Data Release. https://doi.org/10.5066/P9K8OYLG (2022).
- Martin, L.D., Gilbert, B.M., 1978. Excavations at natural trap cave. Trans. Nebr. Acad. Sci. 6, 107–116.
- McEldowney, Roland C., Abshier, John F., Lootens, Douglas J., 1977. Geology of uranium deposits in the Madison limestone little mountain area Big horn county, Wyoming. In: Veal, H.K. (Ed.), Exploration Frontiers of the Central and Southern Rockies: Rocky Mountain Association of Geologists 1977 Symposium, pp. 321–336.
- Min, K., Mundil, R., Renne, P.R., Ludwig, K.R., 2000. A test for systematic errors in ⁴⁰Ar/³⁹Ar geochronology through comparison with U/Pb analysis of a 1.1-Ga rhyolite. Geochem. Cosmochim. Acta 64, 73–98.
- Munroe, J.S., Perzan, Z.M., Amidon, W.A., 2016. Cave sediments constrain the latest Pleistocene advance of the Laurentide ice sheet in the champlain valley, Vermont, USA. J. Quat. Sci. 31 (8), 893–904.
- Murray, A., Thomsen, L.J., Buylaert, J.P., Cuerin, G., Qin, J., Singhvi, A.K., Smedley, R., Thomsen, K.J., 2021. Nat. Rev. 1, 1–31. https://doi.org/10.1038/s43586-021-00068-5.
- Murray, A., Thomsen, K., Masuda, N., Buylaert, J., Jain, M., 2012. Identifying well-bleached quartz using the different bleaching rates of quartz and feldspar luminescence signals. Radiat. Meas. 47, 688–695.
- Murphy, P.J., Lord, T., 2003. Victoria Cave, Yorkshire, UK: new thoughts on an old site. Cave Karst Sci. 30 (2), 83–88.
- Murphy, Phillip J., Smallshire, Robert, Midgley, Christine, 2001. The Sediments of Illusion Pot, Kingsdale, UK: Evidence for Sun-Glacial Utilization of a Karst Conduit in the Yorkshire Dales? Cave and Karst Science, 28, pp. 29–34, 1.
- Naeser, Charles W., 1981. The fading of fission tracks in the geologic environment data from deep drill holes. Nucl. Tracks 5, 248–250.
- Nelson, A.R., Millington, A.C., Andrews, J.T., Nichols, H., 1979. Radiocarbon-dated upper Pleistocene glacial sequence, Fraser valley. Colorado Front Range, Geology 7 (8), 410–414.
- Nelson, M., Gray, H., Johnson, J., Rittenour, T., Feathers, J., Mahan, S., 2015. User guide for luminescence sampling in archaeological and geological contexts. Adv. Archaeol. Pract. 3.
- Nelson, M.S., Rittenour, T.M., 2015. Using grain-size characteristics to model soil water content: a-pplication to doserate-calculation for luminescence dating. Radiat. Meas. 81, 142–149
- Olley, J., Murray, A.S., Roberts, R.G., 1997. The effects of disequilibria in uranium and thorium decay chains on burial dose rates in fluvial sediments. Quat. Sci. Rev. 15 (7), 751–760. https://doi.org/10.1016/0277-3791(96)00026-1.
- Panno, S.V., Greenberg, S.E., Weibel, C.P., Gillespie, P.K., 2004. Guide to the Illinois caverns state natural area: Illinois state geological survey. GeoSci. Educ. Ser. 19, 106.
- Peale, A.C., 1893. The Paleozoic section in the vicinity of Three Forks, Montana, with petrographic notes by G. P. Merrill, U.S. Geol. Surv. Bull. 110, 56.
- Pérez-González, A., Parés, J.M., Gallardo, J., Aleixandre, T., Pinilla, A., 1999. Geología y estratigrafía del relleno de Galería de la Sierra de Atapuerca (Burgos). In:

- Carbonell, E., González, A.R., Fernández-Lomana, J.C.D. (Eds.), Atapuerca: Ocupaciones Humanas y Paleoecología del Yacimiento de Galería, Arqueología en Castilla y León, 7, pp. 31–42.
- Personius, S.F., Mahan, S.A., 2000. Paleoearthquake recurrence on the East Paradise fault zone, metropolitan Albuquerque, New Mexico. Bull. Seismol. Soc. Am. 90 (2), 357–369.
- Peterson, J.A., 1984. Stratigraphy and Sedimentary Facies of the Madison Limestone and Associated Rocks in Parts of Montana, Nebraska, North Dakota, South Dakota, and Wyoming. U.S. Geological Survey Professional Paper 1273-A, p. 34.
- Porat, N., 2006. Use of magnetic separation for purifying quartz for luminescence dating. Ancient TL 24.
- Porat, N., Amit, Zilberman, E., Enzel, Y., 1997. Luminescence dating of fault-related alluvial fan sediments in the southern Arava Valley, Israel. Quat. Sci. Rev. 16 (3–5), 397–402.

Rowlett, R. M. 1980. Unpublished report.

- Sandberg, C.A., Klapper, G., 1967. Stratigraphy, age, and paleotectonic significance of the cottonwood Canyon member of the Madison limestone in Wyoming and Montana. In: Contributions to General Geology, 1251-B. U.S. Geological Survey Bulletin, pp. B1–B70.
- Sando, W.J., 1974. Ancient solution phenomena in the Madison limestone (Mississippian) of North-central Wyoming: U.S. Geol. Surv. Jpn. Rep. 2, 133–141.
- Sando, W.J., 1976. Mississippian history of the northern Rocky Mountains region: U.S. Geol. Surv. Jpn. Rep. 4 (3), 317–338.
- Sando, W.J., 1988. Madison Limestone (Mississippian) Paleokarst. Springer-Verlag, Paleokarst, pp. 256–277.
- Schmitt, A.K., Clementz, M.T., Chamberlain, K.R., 2021. Natural Trap Cave tephra correlation to Yellowstone using U-series (230Th/238U) dates and oxygen isotopes of zircon and chemical composition of adherent glass. This issue.
- Schwartz, Henry, Rink, W. Jack, 2001. Dating methods for sediments of caves and rockshelters with examples from the Mediterranean Region. Geoarchaeology 16 (4), 355–371.
- Sloss, L.L., 1963. Sequences in the cratonic interior of North America. Geol. Soc. Am. Bull. 74, 93–114.
- Sonnenfeld D, M, In M. W. Longman and M. D. Sonnenfeld, eds., Paleozoic Systems of the Rocky Mountain Region. Rocky Mountain Section,, 1996. Sequence Evolution and Hierarchy within the Lower Mississippian Madison Limestone of Wyoming. SEPM (Society for Sedimentary Geology) 165–192.
- Spooner, N., 1994. On the optical dating signal from quartz. Radiat. Meas. 23, 593–600. Stock, G.M., Riihimaki, C.A., Anderson, R.S., 2006. Age constraints on cave development and landscape evolution in the Bighorn Basin of Wyoming, USA. J. Cave Karst Stud. 68 (2), 76–84.
- Veres, D., Cosac, M., Schmidt, C., et al., 2018. New chronological constraints for middle palaeolithic (MIS 6/5-3) cave sequences in eastern Transylvania, Romania. Quat.
- Int. 485, 103–114. https://doi.org/10.1016/j.quaint.2017.07.015.
 Wang, Xiaoming, Martin, Larry D., 1993. Natural trap cave. Natl. Geogr. Res. Explor. 9
 (4), 422–435.
- Westgate, J.A., 1989. Isothermal plateau fission track ages of hydrated glass shards from silicic tephra beds. Earth Planet Sci. Lett. 95, 226–234, 1989.
- White, William B., 2007. Cave sediments and paleoclimate. J. Cave Karst Stud. 69 (1), 76–93.
- Wintle, A.G., Huntley, D.J., 1979. Thermoluminescence dating of a deep-sea sediment core. Nature $279,\,710$ –712.
- Wintle, A.G., Murray, A.S., 2000. Luminescence dating of quartz using an improved single-aliquot regenerative-dose protocol. Radiat. Meas. 32, 57–73.
- Wood, John R., Forman, S.L., Everton, D., Pierson, J., Gomez, J., 2009. Lacustrine sediments in Porter Cave, Central Indiana, USA and possible relation to Laurentide ice sheet marginal positions in the middle and late Wisconsinan. Palaeogeogr. Palaeoclimatol. Palaeoecol. 298 (3–4), 421–431. https://doi.org/10.1016/j. palaeo.2010.10.033.
- Zakrzewski, R., 1975. Pleistocene stratigraphy and paleontology in western Kansas: the state of the art, 1974. Univ. Michigan Pap. Paleontol. 12, 121–128.